

Influence of sintering on CeZrO₄ nano powders prepared for high-k dielectric applications

Mohammad Hayath Rajvee^a, P. Rajesh Kumar^b, Y. Srinivasarao^c

^aCenter for Nanotechnology, Andhra University College of Engineering (A), Andhra University, Visakhapatnam

^bDepartment of Electronics and Communication Engineering, Andhra University College of Engineering (A), Andhra University, Visakhapatnam- 530003

^cDepartment of Instrument Technology, Andhra University College of Engineering (A), Andhra University, Visakhapatnam- 530003

Abstract:—The consequence of milling time and sintering on the size of particles, bandgap and crystalline structure was investigated by milling the pre-sintered and non-sintered powders using dual jar high energy ball milling. XRD [Philips X'pert] results has confirmed the formation of composite this result was further correlated with EDS results taken from FESEM[JEOL JSM-7100F]. The powders prepared were analysed for their bandgap [Ocean Optics-DH-2000-BAL] UV-Visible spectroscopic analyser. There was a deterioration of 41.08% in bandgap which can be attributed to the pre synthesis sintering of the material.

Keywords—sintering, bandgap, ball milling, dielectrics, high-k

I. INTRODUCTION

In the present day microelectronic industry, there is requirements of high-*k* materials for functioning as gate dielectric in advanced MOS circuits [1]. In current ultra large scale integrated (ULSI) circuits, the scaling of devices has reached a limit where SiO₂ gate dielectrics are incapable to stop direct tunneling of electrons from gate metal to the channel arising in an increase in gate leakage currents[2-4]. Therefore, to overcome the gate delay and other related issues many researchers are working on alternate high dielectric constant (high-*k*) oxides [5]. High *k* materials developed must be good in their thermal stability, permeability, quality of film and should have lower interfacial traps, optimal compatibility with fabrication of MOS devices and long-term reliability. Owing to their credible properties, such as large critical electric field, good thermal conductivity, high electron mobility and stability, wide band gap (WBG) semiconductors are being seen as promising materials in substituting Si for devices based on high-power metal oxide semiconductor (MOS) [6,7].

CeO₂ can be said as remarkable gate dielectric material for MOS devices because of its stable chemical properties, ease of processing, compatibility with silicon, high dielectric constant and high oxygen diffusivity with low leakage current density [8]. Rare-earth cerium oxide(CeO₂) has garnered significant consideration as a substituting gate oxide to SiO₂ with its cubic fluorite structure, high dielectric constant ($k = 26$) and large band gap (6 eV). The electric field imposed in the gate oxide may be suppressed by a factor of (3.9) due to the introduction of CeO₂ when compared with SiO₂ [9,10]. Cerium oxides (CeO₂ and Ce₂O₃) do have good oxygen storage capacity. Zr has been incorporated into CeO₂ as to improve thermal stability and also to evaluate the lattice mismatch between Si and CeO₂ enabling one to reduce the interface trap density further [11]. After high-temperature annealing, Zr silicate or ZrO₂ phases are produced which both maintain the value of the dielectric constant, if Zr does not react with CeO₂ to form CexZr_{1-x}O₂ ternary oxide. Zirconium

oxide with its high dielectric constant ~15–22, a high breakdown field ~15–20 MV/cm, is thus a promising candidate[12]. In this study consequence of sintering on bandgap of powders before being milled was analysed in comparison with the powders that were milled as received.

II. EXPERIMENTATION

Cerium oxide (99.9% pure), Zirconium Oxide (99.9% pure) powders used for the present work are supplied by Sigma Aldrich, USA. Two sets of powders in 1:1 molar ratio were tested in this work. One combination of powders was sintered at 800°C for one hour while another combination of powders is loaded as received. The powders were loaded in 125 ml zirconia jars along with (ϕ3mm) Zirconia balls. The powders were milled in high energy ball milling machine (Retsch make) maintaining ball to powder ratio of 10:1 at 800rpm. The powders were milled for different milling times of 2h, 3h and 4h with an interval of 10 min for every 1h. Samples were collected in every interval to investigate the effect of milling time on the bandgap. The very fine powders are prone to stick to the surface of balls and the inner walls of the jar during milling. The degradation of milling efficiency is overcome by manually spalling the consolidated powders from the balls and the jar in every interval. Milled Powders are then heat treated at 800°C for 2h. High-energy ball milling of ceramic powders can reduce the average crystallite sizes from the μm regime down to some nm.

The prepared powder was characterized by XRD [Philips X'pert] and FESEM [JEOL JSM-7100F] to confirm the size and crystallinity of the particles collected in every interval. As prepared powders were suspended in methanol and then sonicated for 10 min in an ultrasonic bath to achieve uniform dispersion of the particles which were then subjected to UV-Visible spectroscopy [Ocean Optics-DH-2000-BAL] for bandgap analysis.

III. RESULTS AND DISCUSSION

Powder X-ray diffraction data was collected with a Philips x'pert system using CuKα radiation ($\lambda = 1.5418 \text{ \AA}$) at 45KV and step size of 0.008Å by placing the samples in aluminum holders. No change was observed in the Monoclinic structure of ZrO₂ which is consistent with the studies of Songlin Li et al etc. [5]. These results were analyzed using match! 3 software. Crystallite size was measured using Scherrer formula,

$$D = \frac{K\lambda}{\beta \cos\theta} \tag{1}$$

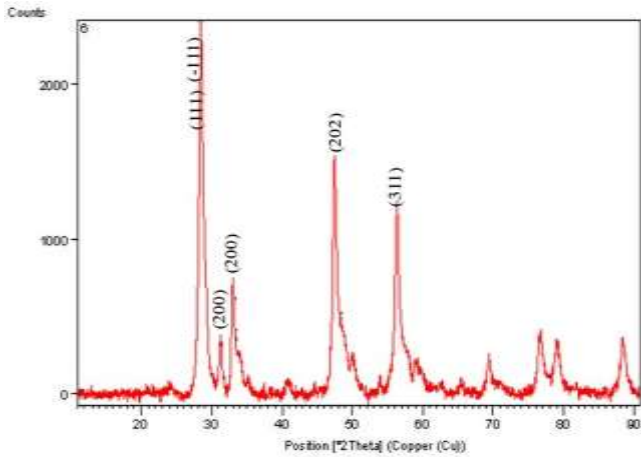


Fig. 1. XRD image of CeZrO4

where, K is Scherrer constant=0.94, λ is X-ray wavelength = 0.15418nm and β is width of the XRD peak after corrections concerning instrumental broadening, θ is diffraction angle gives the average crystallite size D as 39.8nm.

XRD peaks were corrected for the effects of the Kα2 radiation and instrumental broadening. XRD pattern shown in fig. 1. discloses the presence of Cerium and Zirconium peaks (111), (200), (311) and (-111), (200), (202). All the peaks observed in this analysis are consistent with the existing work

by songlin Li et.al. [5] FESEM images were taken in JSM-7100F at 100000x magnification and beam voltage of 10KV with a working distance of 6mm. Figure 2(a),(b)&(c) are pertaining to the non-sintered sample showing the particle size variation with milling time. A constant reduction of particle size was observed from the images. Figure 2(a) shows particles of 2h milled powder having particle size around 117nm which may be considered in micron size. The bandgap of this powder was calculated to be 1.78 (its absorption spectra is shown in fig 6(a), where figure 2(b) shows particles of 3 h milled powder has reached to nanoscale showing approximately 40nm particle size. Reduction in particle size have raised the bandgap to 2.10. The subsequent image of figure 2(c) was taken at 400000x magnification showing 22 and 17 nm size particles, and a raise in bandgap of the material of smaller particles was also observed to be 2.79 calculated from the absorption spectra of figure 6(a). It can be observed from FESEM images of figure 3 that; particle size reduction was quick from micro to nanoscale while it has taken comparatively longer time for further reduction in nanoscale. Sintering may affect quicker particle size reduction which was evident from the FESEM images shown in figures 3 (a), (b) and (c) of pre-sintered samples that the powder reaches to nano scale in the first two hours. Whereas its size was not much considerably lowered even after milling for another two hours (the minimum particle sizes are marked in the images). This effect was attributed to the pre-sintering effect on particles size.



Fig. 2. FESEM images of non-sintered powders after milling time of (a) 2 h, showing particle size 117nm (b) 3 h, showing particle size 39.8nm (c) 4 h, showing particle size 17.7nm

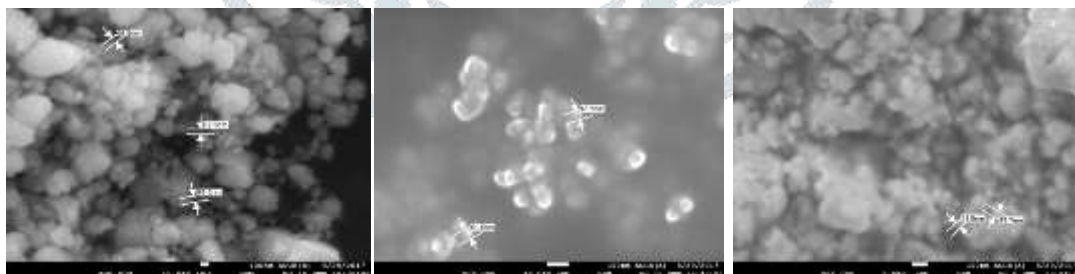


Fig. 3. FESEM images of pre-sintered powders after milling time (a) 2 h showing particle size 62.5nm (b) 3 h showing particle size 43nm (c) 4 h showing particle size 41nm

Table1. and figure 4. are results taken from Oxford’s EDS detector attached to FESEM machine. The quantitative elemental analysis was carried out by INCA software. This gave the evidence that the composition has reached the required stoichiometry. UV-VIS spectroscopic analysis has been conducted on the pre- sintered and non-sintered samples in [OceanOptics-DH-2000-BAL] spectroscopic analyzer. Bandgaps of samples calculated using

$$E_g = \frac{12400}{\lambda A^\circ} \text{ eV}$$

where, λ is the wavelength of the maximum absorption.

The absorption spectra of non-sintered samples are shown in Figure 6(a) and at the maximum absorption in the figure the corresponding atom was marked. The maximum values of

absorption corresponding to each sample are shown in graph of figure 5. Similarly figure 6(b) shows the absorption spectra of powders sintered for different milling times each marked at the highest peaks for calculating the bandgap of the materials. A large deterioration in the bandgap with milling time of pre-sintered powders was identified compared to that of non-sintered powders.

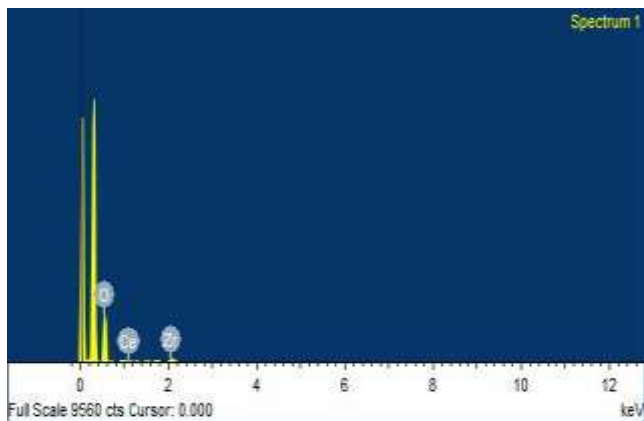


Fig. 4. EDS spectra showing quantity of elements

Table 1. Quantitative elemental analysis obtained from EDS results

Element	Weight%	Atomic%
O K	1.35	94.18
Zr L	0.23	2.87
Ce L	0.37	2.95
Totals	1.96	

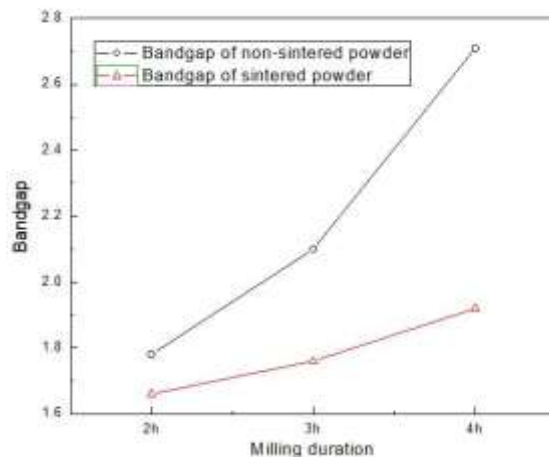


Figure 5: Bandgap comparison curves of sintered and non-sintered materials

Each curve of figures 6 (a) and (b) were pertaining to samples milled for 2h, 3h & 4h respectively were marked in the mages. From figure 5, it can be observed that the bandgap was fairly improving in the material which were milled as received. Whereas, bandgap improvement with milling time in the sintered powders were observed very poor. A large minimum to maximum bandgap difference was achieved in directly loaded powders and a little improvement in the sintered powders.

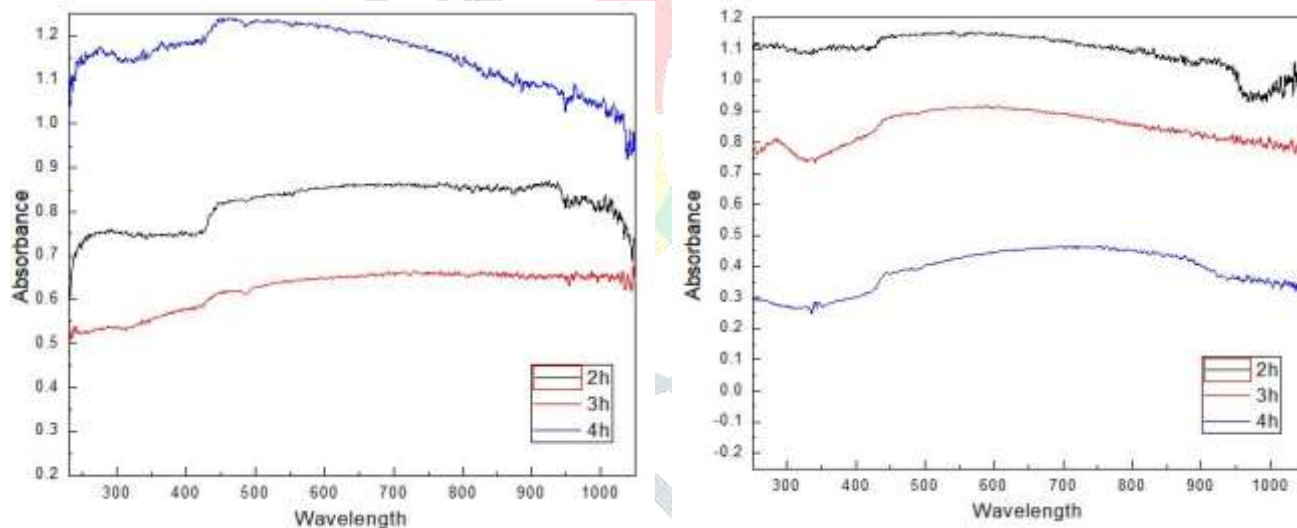


Fig. 6. UV-Vis spectroscopic results of (a) Non-sintered powders (b) Pre-sintered powders

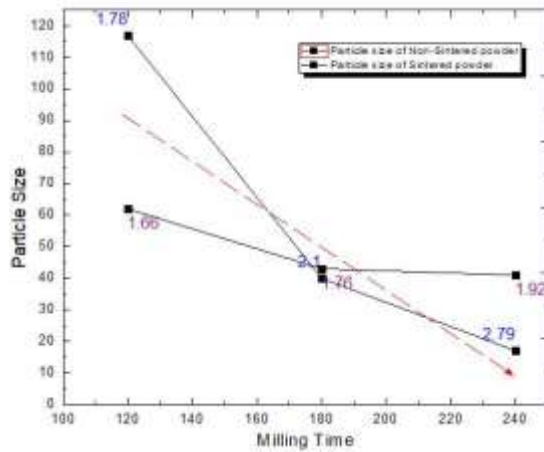


Fig. 7.: Milling time Vs Particle size

Figure 7 shows effect of milling time on particle size and effect of particle size on the bandgap of material. The dotted arrow line showing the bandgap improvement depending upon the milling time as well as particle size. In this work we have demonstrated that amorphous material size can be reduced faster than the heat treated material.

IV. CONCLUSION

A large deterioration of 41.08% was seen in the bandgap of materials that were sintered at a temperature of 800°C for 1 h before milling. The sizes of particles in pre-sintered powders are found to be larger than that in non-sintered powders though milled for the same time. This can be attributed to the formation of crystallinity of the powder that delayed the particle size reduction with respect to milling time. Maximum bandgap achieved for sintered and non-sintered powders are 1.92eV and 2.79eV after four hours of milling time, as shown in figures 6 (a)&(b) and minimum particle sizes were 43nm and 17.2nm as shown in figure 2 and figure 3. Pre-synthesis sintering has affected prominently the electrical nature of the material. As a future work bandgap analysis can be done on powders by milling them for longer times (Graphs depict the possibility of improvement in the

bandgaps further). Materials with wide bandgap find their appropriate applications in many fields particularly in the industry of MOS devices.

V. REFERENCES

- [1] F. Varsano, F. Decker, E. Masetti, F. Cardellini, A. Licciulli, "Optical and electrochemical properties of cerium-zirconium mixed oxide thin films deposited by sol-gel and r.f. sputtering, *Electrochimica Acta* 44 (1999) 3149–3156
- [2] D.L. Zhang, "Processing of advanced materials using high-energy mechanical milling", *Progress in Materials Science* 49 (2004) pp: 537–560.
- [3] ANIL G KHAIRNAR and ASHOK, et al. "Sol-gel deposited ceria thin films as gate dielectric for CMOS technology", *Bull. Mater. Sci.*, Vol. 36, (2013)pp. 259–263.
- [4] Alessandro Trovarelli, Francesca Zamar, Jordi Llorca, Carla de Leitenburg, Giuliano Dolcetti, and Janos T. Kis, "Nanophase Fluorite-Structured CeO₂-ZrO₂ Catalysts Prepared by High-Energy Mechanical Milling", *JOURNAL OF CATALYSIS* 169, (1997)pp:490–502
- [5] Songlin Li, Lei Wang, Yuming Xiong, Gyuyeol Bae, and Changhee Lee, "Amorphization of ZrO₂ + CeO₂ Powders Through Mechanical Milling for the Use of Kinetic Spray" *JMEPEG* (2013) 22:3717–3722.
- [6] P. Lacorrel and R. Retoux, "First Direct Synthesis by High Energy Ball Milling of a New Lanthanum Molybdate", *JOURNAL OF SOLID STATE CHEMISTRY* 132, 443–446 (1997)
- [7] Jinshu Wang, Shu Yin, Masakazu Komatsu, Tsugio Sato, "Lanthanum and nitrogen co-doped SrTiO₃ powders as visible light sensitive photocatalyst", *Journal of the European Ceramic Society* 25 (2005) 3207–3212
- [8] Chun Zhao¹, Ce Zhou Zhao, et al. "Grain size dependence of dielectric relaxation in cerium oxide as high-k layer", *Nanoscale Research Letters*, vol.8.(2013)pp:2-10
- [9] Hossein Mahmoudi Chenari, Hadi Fallah Moafi, et al. "A study on the microstructural parameters of Zn (1-x)LaxZrxO nanopowders by X-ray line broadening analysis", *Materials Research*, vol. 19. (2016)pp:548-554.
- [10] Way Foong Lim Kuan, Yew Cheong, et al. "Influence of post-deposition annealing in oxygen ambient on metal-organic decomposed CeO₂ film spin coated on 4H-SiC" *J Mater Sci: Mater Electron*, vol.23 (2012) pp:257–266.
- [11] B. Elidrissi, M. Addou, M. Regragui, C. Monty, A. Bougrine, A. Kachouane, "Structural and optical properties of CeO thin films prepared by spray pyrolysis, *Thin Solid Films* 379 (2000)pp:23-27
- [12] Wenzhi Huang, Jili Yang, Chunjie Wang, Binglin Zou, Xiangsheng Meng, Ying Wang, Xueqiang Cao, Zhen Wang, "Effects of Zr/Ce molar ratio and water content on thermal stability and structure of ZrO₂-CeO₂ mixed oxides prepared via sol-gel process", *Materials Research Bulletin* 47 (2012) 2349–2356.